Available online at www.sciencedirect.com
ScienceDirect
Journal of the European Ceramic Society 28 (2008) 1185–1190
www.elsevier.com/locate/jeurceramsoc

# Tape casting and reaction sintering of titanium–titanium oxide–nickel oxide mixtures

M.D. Snel [a,b], F. Snijkers [b], J. Luyten [b], A. Kodentsov [a], G. de With [a,*]

[a] *Laboratory of Materials and Interface Chemistry, Technische Universiteit Eindhoven (TU/e), PO Box 513, 5600 MB Eindhoven, The Netherlands*
[b] *Materials Department, Flemish Institute for Technological Research (VITO), Boeretang 200, 2400 Mol, Belgium*

Received 29 August 2007; received in revised form 29 October 2007; accepted 2 November 2007
Available online 14 January 2008

**Abstract**

Suspensions of a powder mixture of titanium–titanium oxide–nickel oxide were tape cast. Analysis of the green tape showed an increase in Young's modulus and tensile strength with increasing powder volume content $\phi$ up to 28 vol%; at higher $\phi$ the properties decreased due to the formation of flaws in the green tape. The elongation of the green tape decreases continuously with increasing $\phi$. Green tapes were laminated and were reactively sintered at 1350 °C to form a composite of TiO–$NiTi_2$–$Ni_3Ti$ with a porosity of ~5%. The wetting of TiO by $NiTi_2$ prevented the TiO grains of forming a highly connected network, despite TiO making up 50% of the volume. The mixed intermetallic phases $NiTi_2$ and $Ni_3Ti$ did form a continuous network. The three point bending strength of the composites was 121 MPa.


*Keywords:* Tape casting; Reaction sintering; TiO; NiO; Ti

## 1. Introduction

Tape casting is widely used by the industry for making large thin sheets of ceramic materials for the fabrication of substrates, multilayer products, piezoactuators, sensors, etc.[1–4] Traditionally, tape casting involves organic liquids as dispersing medium, but currently the trend is to move away from organic solvents towards water based systems. The main reasons for using water based systems are the low toxicity, the low cost and the reduction of environmental risks.[4] The disadvantages of using water based systems are, however, the slower drying rate and the higher possibility of cracking during drying as compared to the commonly used organic solvent based systems.

Reactive forming techniques have been used to replace traditional processing for several reasons.[5] The low-cost starting materials, low energy input, high purity and (near)-net-shape capabilities are the most important ones. In general ceramics made by reactive forming techniques, like reaction bonded silicon carbide (RBSC) and reaction bonded silicon nitride (RBSN), use solid/gas, solid/liquid or liquid/gas reactions. The reaction bonding of aluminium oxide (RBAO), introduced in the early 1990s, uses the reaction of Al with oxygen to form fully dense aluminium oxide ceramics.[6,7]

In 1997,[8] the aluminium aluminide alloys (3A) were introduced. In this process a body is formed containing an intermetallic aluminide or an aluminium alloy, and a ceramic phase. The reaction takes place in a non-oxidizing environment. In the green body, aluminium metal is finely distributed together with a metal oxide. During sintering, the aluminium will reduce the metal oxide, forming a metal aluminide or metal aluminium alloy and a ceramic phase, which normally will be $Al_2O_3$, but which can also be a mixed oxide.

This same principle can be applied to titanium, which will form titanium titanide alloys (TTA). Although titanium is less reactive than aluminium, most other elements will be reduced by the reaction:

$$\mathrm{Ti} + \mathrm{MeO}_x \rightarrow \mathrm{Ti}_k\mathrm{O}_l + \mathrm{Ti}_m\mathrm{Me}_n$$

The TTA process in the Ni–Ti–O system is possible in the triangle between the line Ti–NiO and $TiO_2$ (Fig. 1).[9] The addition of $TiO_2$ is mainly to control the exothermic reaction, but in contrast to the 3A process, where the $Al_2O_3$ does not react, it is

* Corresponding author. Tel.: +31 40 2472770; fax: +31 40 2445619.
*E-mail address:* G.dewith@tue.nl (G. de With).

0955-2219/$ – see front matter © 2007 Elsevier Ltd. All rights reserved.
doi:10.1016/j.jeurceramsoc.2007.11.001

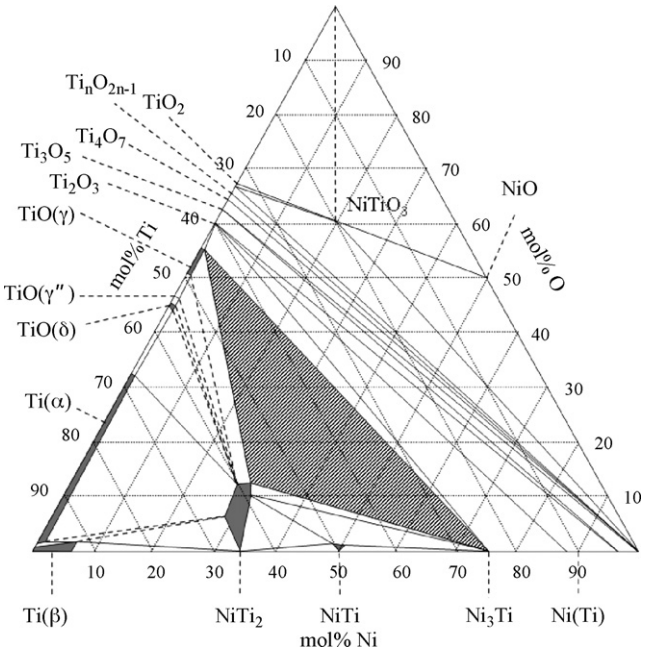


Fig. 1. Phase diagram of the nickel–titanium–oxygen system. The hatched triangle indicates the working area.

possible that the $TiO_2$ will take part in the reaction due to the presence of a range of different titanium oxides, e.g. TiO, $TiO_2$, $Ti_2O_3$ and the Magnelli phases $Ti_nO_{2n-1}$. It should be noted that it is not possible to obtain the shape memory and superelastic NiTi, since the oxygen content of the mixture will prevent its formation.

The hatched area in the ternary phase diagram in Fig. 1 was chosen in view of the possible use of the composite for biomedical components, similar to $Ni_3Ti$–$TiC_x$ composites[10]; for compositions more to the right in the diagram, the presence of elemental nickel would prohibit the use of the resulting material for biomedical applications. For compositions in the lower left corner (Ti–$NiTi_2$), the resulting composites would not have a ceramic phase, and loose the potential benefits of ceramics over metals and intermetallics, like wear and oxidation resistance. Of the materials in the two remaining regions (TiO–$NiTi_2$–Ti and TiO–$NiTi_2$–$Ni_3Ti$), $Ni_3Ti$[10] and Ti[11] are investigated for use in biomedical applications and $NiTi_2$[12] is an intermetallic compound with a reasonably good combination of ductility and mechanical properties; the region TiO–$NiTi_2$–$Ni_3Ti$ was chosen for this work. Due the much higher melting point of $Ni_3Ti$ ($T_m = 1380\,^\circ C$) than $NiTi_2$ ($T_m = 984\,^\circ C$) the final composition was chosen near the line TiO–$Ni_3Ti$.

## 2. Experimental procedures

The experimental procedure is depicted in Fig. 2.

A mixture of 100 g consisting of titanium dioxide (T-1193, Absco Ltd., UK, ~75 μm), nickel oxide (N-1042, Absco Ltd., UK, typically 5 μm or less) and titanium (T-1147, Absco Ltd., UK, 11–74 μm) was ball milled in polyamide jars in acetone and yttria stabilized zirconia milling balls for 8 h. The coarse $TiO_2$ was chosen to increase the milling action on the titanium powder. After milling the $TiO_2$ had a size of ~20 μm. The mixture was chosen in the hatched triangle shown in the ternary phase diagram of nickel–titanium–oxygen in Fig. 1.[9]

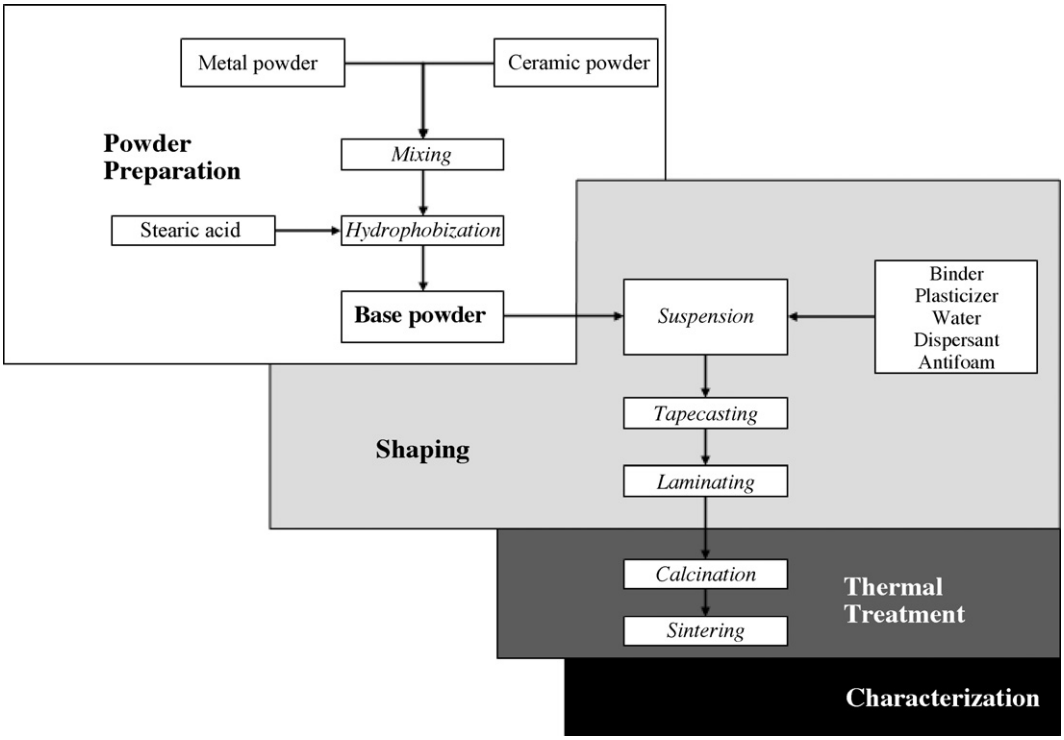


Fig. 2. Process flow of tape casting of titanium–titanium oxide–nickel oxide mixture. Italic font indicates processing steps, materials added during the processing are indicated by normal font.

The next step in the process was the hydrophobization of the powder with stearic acid. Two grams of stearic acid was dissolved in 125 g acetone of ∼40 °C and added to 100 g of the powder mixture and subsequently dried in a Rotavapor (RE 111, Büchi, Switzerland) at 55 °C and low pressure, resulting in the starting powder. In the next step the slurry was prepared by premixing water, dispersant (Triton X-114, FLUKA, Germany) and antifoaming agent (DB-310, Dow Corning, USA), followed by the simultaneous addition of the starting powder, binder (Duramax B-1014, Hoechst, Germany) and plasticizer (polyethylene glycol (PEG) 400, Merck, USA). To prevent cracking an amount of water as small as possible was used. However, this means that it was not possible to disperse the powder prior to the addition of the (water-based) binder, which is usually done in tape casting. The mixture was subsequently ball milled for 10 min at low speed to create a homogeneous slurry, avoiding stirring too vigorously or too long to destroy the stearic acid coating. In the final preparation step, the slurry was deaired in rough vacuum.

Tape casting (TTC-1200, Tape Casting Warehouse, USA) was done with a gap height of 0.50 mm, width 10 cm and a carrier film speed of 28 cm/min using a single doctor blade. After drying in air, the binder burnout was combined with the calcination of the compact and was done at 20 °C/h up to 500 °C in air. Sintering (Torvac, Centor Industries, USA) was done in vacuum at 5 °C/min to 1350 °C for 2 h.

The slurry and the slurry components have been characterized by rheological properties (Haake Rheostress RS 100, Germany). The strength of the green tapes has been measured by tensile testing (Instron 1195, Germany) according to DIN 53504 standard. Imaging was done with scanning electron microscopy (SEM, Jeol JSM-840A, Japan). Crystallographic characterization was done with from X-ray diffraction (XRD, Rigaku Geigerflex, Fe Kα, Japan). Differential scanning calorimetry (DSC, Netsch STA 449C Jupiter, Germany) was done on the powder. Three point bending strength of the sintered samples have been measured (Instron 1195, Germany) on two specimens of 9 mm × 0.4 mm with a span of 20 mm and a crosshead speed of 0.5 mm/min in air.

## 3. Results and discussion

The hydrophobization step is crucial to the process. If the amount of stearic acid added is too high, agglomerates will be formed in the final green tape; if it is too low, the surface area of the particles will not be completely covered by the stearic acid and the dispersant cannot function optimally resulting in an unstable suspension. To determine the optimum addition of stearic acid, mixtures have been prepared of powders coated with different amounts of stearic acid and water. The results are shown in Table 1. For no addition of stearic acid the powder will formed a turbid fluid through which no light can pass. The transmitted light intensity increased with increasing amount of stearic acid, indicating an increase in hydrophobicity of the powder. When the stearic acid reached the level of 2.0 wt%, the liquid was clear, the powder completely hydrophobic and will floated on top of the water. Using higher levels of stearic acid does not change the behaviour of the powder.

Table 1
Results of mixing of 2 ml of water and 0.25 g of powder, coated with different amounts of stearic acid

| wt% stearic acid | Result |
|---|---|
| 0.0 | Turbid fluid |
| 0.5 | Dark turbid fluid with some powder floating on top |
| 1.0 | Lightly turbid fluid with powder floating on top |
| 2.0 | Clear fluid with powder floating on top |
| 4.0 | Clear fluid with powder floating on top |
| 7.0 | Clear fluid with powder floating on top |

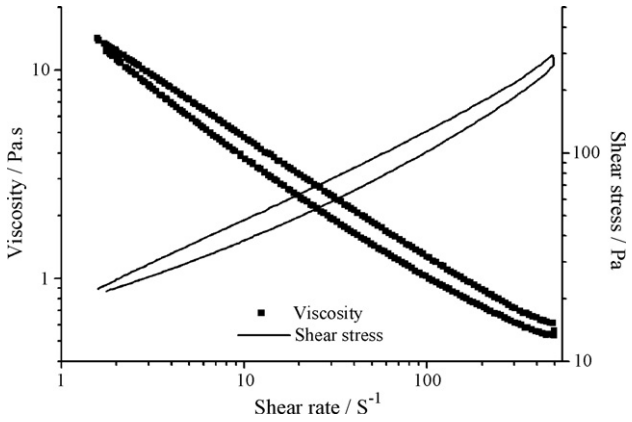


Fig. 3. Shear stress and viscosity of the suspension as function of the shear rate. The volume fraction of powder is 0.28 of the total suspension.

After hydrophobization the powder was mixed with the other constituents to obtain the tape casting suspension. In Fig. 3, the typical viscosity behaviour of the suspension with a powder volume fraction of powder $\phi = 0.28$ is presented as function of the shear rate. The shear thinning behaviour for this mixture is typical for ceramic suspensions and beneficial for tape casting; a low viscosity at high shear rate ensures that the paste will smoothly pass underneath the doctor blade, while a higher viscosity at low shear rate ensures that the paste will stop flowing after it has passed the blade.

Fig. 4 shows the viscosity of the slurries as a function of $\phi$ for different shear rates. As expected, the viscosity increases with

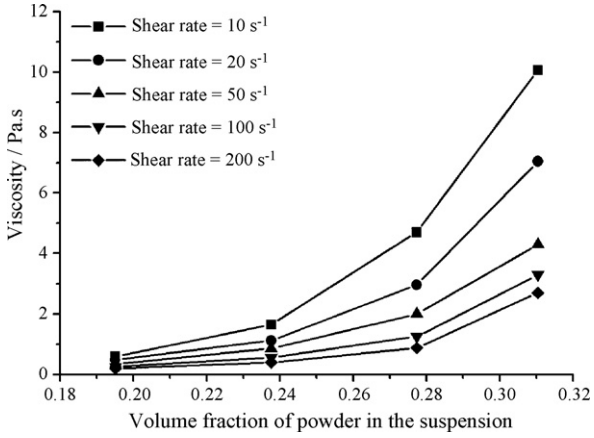


Fig. 4. Viscosity at different shear rates as function of the volume fraction of powder in the suspension.

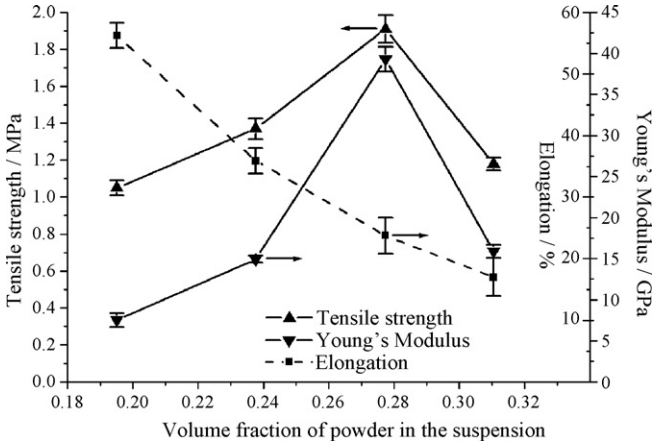


Fig. 5. Maximum tensile stress, Young's modulus and total elongation of the green tapes as function of the volume fraction of powder in the suspension using tensile testing with a crosshead speed of 10 mm/min. The cross section of the samples was 5.8 mm × 0.28 mm.

increasing $\phi$. The viscosity decreases at higher shear rates for all powder volume fractions, as shown in Fig. 3 for $\phi = 0.28$. Although a high $\phi$ is desirable,[1] the accompanying increase in viscosity has an effect on the properties of both the green tape (flexibility, the formation of agglomerates, cracking, etc.) and the final composite (density, flexural strength, etc.). As the viscosity reflects the consistency of the slurry, a high viscosity can result in flaws being introduced in the green tape and a low viscosity can result in the settling of the heavier particles.[13] Common viscosities for tape casting are in the range of 5–25 Pa s. Assuming Couette flow, the shear rate is the ratio between the carrier tape speed (28 cm/min) and the gap height (0.50 mm), which gives a shear rate of 10 $s^{-1}$ for our experiments, indicating that a $\phi = 0.28$ and $\phi = 0.31$ in the slurry are feasible.

To determine the properties of the green tape, the tensile strength, the Young's modulus and the total elongation were measured using tensile testing according to DIN 53504 standard. The sample cross section was 5.8 mm × 0.28 mm. The results are shown in Fig. 5. With increasing volume fraction of the powder in the suspension both the tensile strength and the Young's modulus of the green tape increase up to $\phi = 0.28$, but they decrease for a higher volume fraction. The elongation continuously decreases with increasing $\phi$.

For the green strength a similar behaviour has been shown for the aqueous tape casting of hydroxyapatite.[14] At low binder content, the strength is predominantly determined by the binder matrix, which provides good cohesion of the green tape. Increasing the powder content results in stiffening/strengthening of the green tape and a decrease in elongation. The increase in viscosity due to the increase in $\phi$, as shown in Fig. 4, leads to a tape casting suspension which is difficult to de-air and not homogeneous. The resulting flaws in the green tape are the cause of the lower green strength at higher $\phi$.

For the Young's modulus this behaviour is not expected. For composites the Young's modulus are normally estimated by using the rule of mixtures or models like the Kerner–Uemura–Takayanagi model.[15] Since the Young's modulus of ceramic materials is generally higher than the Young's modulus of the polymer binder, a continuous increase of the Young's modulus is expected with increasing $\phi$. Probably, the introduction of the flaws at higher $\phi$, leading to localized deformation, is responsible for this decrease.

There have been reports of composite materials with a similar trend in Young's modulus in the literature on fillers in polymer matrices.[16] In that case the Young's modulus decreases due to phase separation as a result of differences in hydrophobicity. That is comparable to the situation for our green tapes in which the powder is more hydrophobic than the polymer latex, resulting in the formation of hydrophobic agglomerates. These agglomerates act like stress localizers and reduce the strength of the green tape, even though the agglomerates may be strong enough to increase initially the tensile strength and the Young's modulus.[17]

If the agglomerates and the polymer matrix adhere poorly to each other, the agglomerates effectively act as pores in the polymer matrix, resulting in a structure similar to foam. For foams it is known that the Young's modulus decreases with an increase in pore number and size.[18] Also large weak agglomerates, even if adhesion to the polymer matrix is present, will show many characteristics of pores.[17] Hence, with a low number of agglomerates formed at low solid loadings, the addition of powder to the polymer matrix increases the Young's modulus and above the critical value of $\phi = 0.28$ the formation of agglomerates will reduce the Young's modulus.

Combining the results of the tensile testing and the rheology, at a shear rate of 10 $s^{-1}$ the best properties are obtained using the slurry with $\phi = 0.28$, which results in a viscosity of 4 Pa s during the tape casting process.

Fig. 6 shows the XRD pattern of the powder mixture after milling and the XRD pattern of the sintered and ground Ni–Ti–O composite. The initial powder mixture clearly shows the three original phases Ti, $TiO_2$ and NiO, indicating that no reaction takes place during the ball milling. The XRD pattern of the sintered Ni–Ti–O composite shows the three phases which are expected for the region selected in the phase diagram: TiO, $NiTi_2$ and $Ni_3Ti$. No other phases were detected. In particular, no free Ni was present, which is a requirement for biomedical applications. It should be noted that distinguishing between TiO and

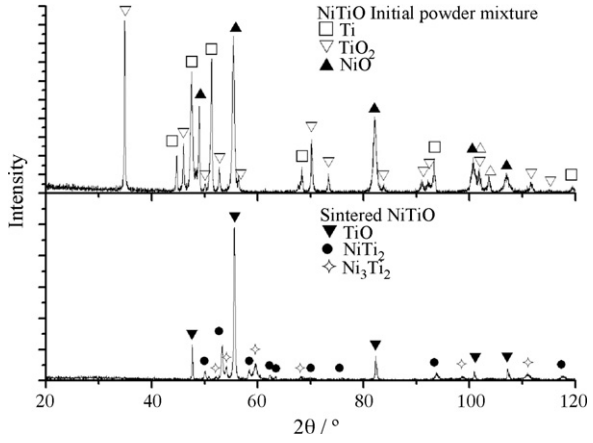


Fig. 6. XRD pattern of the initial Ni–Ti–O powder mixture (above) and sintered and ground Ni–Ti–O composite (below). Fe radiation was used (λ = 1.93604 Å).

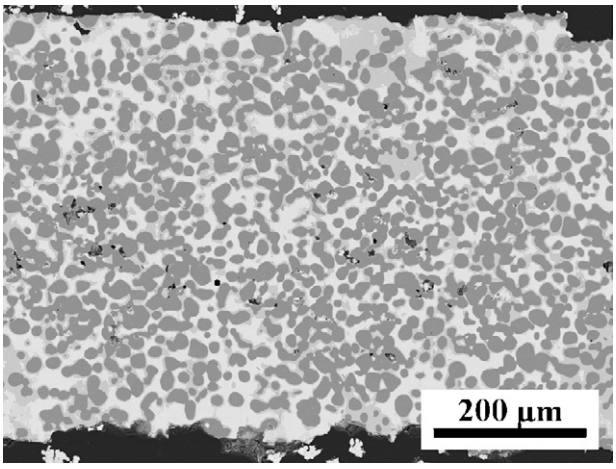


Fig. 7. Backscattered SEM (150×, 15 kV) image of the microstructure of the sintered Ni–Ti–O composite using $\phi = 0.28$. The dark grey phase is TiO, the grey phase is $NiTi_2$ and the light grey phase is $Ni_3Ti$. The pores are black.

NiO is nearly impossible, since these compounds have the same structure (cubic, rock salt) and nearly the same lattice parameters: NiO has lattice constant of 0.4177 nm[19] and TiO a lattice constant of 0.4166–0.4187 nm, depending on the ratio O/Ti.[20,21] DSC measurements showed for all compositions a sharp, single exothermic peak at 750 °C, indicating that the final phases are formed in a single reaction.

In Fig. 7 a SEM picture is presented of the microstructure of the Ni–Ti–O composite after sintering at 1350 °C, using the slurry with $\phi = 0.28$. The presence of a three-phase system is clear: the dark phase is TiO, the grey phase is $NiTi_2$ and the light coloured phase is $Ni_3Ti$. Image analysis shows that the amounts of TiO, $NiTi_2$ and $Ni_3Ti$ are 50%, 25% and 20% by volume, respectively, while the porosity covers 5%. With 50% TiO, it was expected that the ceramic phase would form a clear interpenetrating network with the (mixed) intermetallic phase. However, the TiO phase does not appear highly connected. Nevertheless, a quite homogeneous microstructure is obtained.

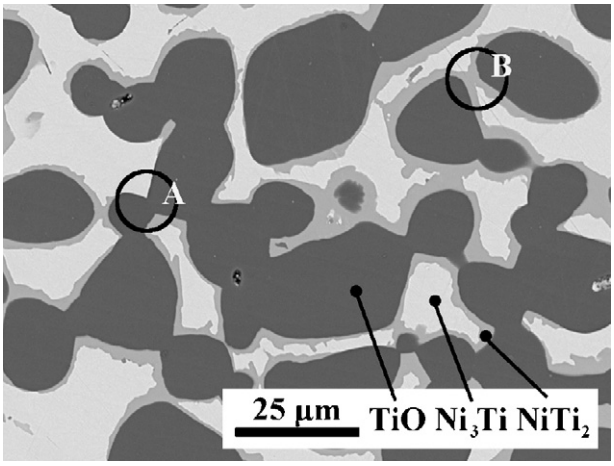


Fig. 8. SEM (1000×, 15 kV) image of the microstructure of the Ni–Ti–O system composite after sintering. The dark grey phase is TiO, the grey phase is $NiTi_2$ and the light grey phase is $Ni_3Ti$.

In Fig. 8 the microstructure of the Ni–Ti–O composite is shown in more detail. From this figure it becomes clear that the TiO phase is nearly always in contact with the intermetallic $NiTi_2$, and that $Ni_3Ti$ fills up the space between the ceramic grains. This microstructure indicates that $NiTi_2$ is a good wetting agent for TiO.

This microstructure resulted due to five reasons. (1) The particle size of $TiO_2$ is about 20 µm after milling, which makes sintering of the ceramic phase at low temperatures unlikely. However, using a starting mixture with 1 µm $TiO_2$ resulted in a similar microstructure.[22] (2) According to the DSC experiments a single sharp exothermic peak is observed at 750 °C. In this reaction the final products TiO, $NiTi_2$ and $Ni_3Ti$ are formed. (3) At 984 °C the $NiTi_2$ melts and will wet the TiO particles. (4) At 1350 °C, which is just below the melting point of $Ni_3Ti$, the $Ni_3Ti$ phase will fill up the voids between the TiO particles, wetted by the $NiTi_2$. (5) At locations where the $NiTi_2$ did not completely wet the TiO particles or the TiO was already in contact, necking results, see for instance location A in Fig. 8. However, in other locations, see location B, necking is prevented by $NiTi_2$.

Three point bending (3pb) testing has been conducted on two samples of the sintered composite. The average 3pb strength is 121 MPa. Using different sintering schemes yielded specimens with similar densities and similar strength (113 MPa). The precise profile is thus not the prime-determining factor for the strength, although the low number of samples makes the result not very accurately.

Investigations are planned to check whether varying milling time, using different starting powders, adapting the sintering profile, along with investigating the effect of doping the material, with e.g. B, will change the wetting behaviour of the ceramic phase by the intermetallic phase.

## 4. Conclusions

It has been shown that it is possible to coat a mixture of titanium–titanium oxide–nickel oxide with stearic acid to render it hydrophobic. The optimum amount of stearic acid was 2 g per 100 g of powder. Analysis of the green tape showed an increase in Young's modulus and tensile strength up to a volume fraction $\phi$ of 0.28. At higher $\phi$ the Young's modulus and tensile strength dropped due to the formation of flaws in the green tape. The elongation continuously decreases with higher $\phi$, as expected.

This powder mixture was successfully tape cast and sintered at 1350 °C. The resulting material showed 5% porosity and has a continuous intermetallic phase, a mixture of $NiTi_2$ and $Ni_3Ti$. Despite making up 50% of the volume, the ceramic phase TiO is not highly connected. This low connectivity of the ceramic phase is probably due to the wetting of the $NiTi_2$ phase, preventing the growth of a highly connected TiO network. In locations where the $NiTi_2$ did not wet the TiO grains or where the TiO was in contact before wetting, necking is observed. The wetting behaviour of $NiTi_2$ can possibly influenced by adding a fourth element as wetting agent or changing process parameters.

For biomedical applications two essential requirements are the absence of free Ni and sufficient strength. For our composites

free Ni was not detected while the three-point bending strength of the composite (121 MPa) is comparable to the strength of femur bone.

## Acknowledgements

This research is funded by the doctorate program of the Flemish Institute for Technological Research (VITO). The authors wish to acknowledge Jos Cooymans, Jean van Hoolst and Ivo Thijs at VITO, for their help in preparing the samples. Furthermore, Marco Hendrix (TU/e) and Myrjam Mertens (VITO) are acknowledged for their with the XRD and SEM measurements. Willy Hendrix (VITO) is acknowledged for performing the three point bending test and tensile testing.

## References

1. Hotza, D. and Greil, P., Review: aqueous tape casting of ceramic powders. *Mater. Sci. Eng. A*, 1995, **202**, 206–217.
2. Zhang, Y. and Binner, J., Tape casting aqueous alumina suspensions containing a latex binder. *J. Mater. Sci.*, 2002, **37**, 1831–1837.
3. Chartier, T. and Rouxel, T., Tape-cast alumina-zirconia laminates: processing and mechanical properties. *J. Eur. Ceram. Soc.*, 1997, **17**, 299–308.
4. Bitterlich, B., Lutz, C. and Roosen, A., Rheological characterization of water-based slurries for the tape casting process. *Ceram. Int.*, 2002, **28**, 675–683.
5. Claussen, N., Janssen, R. and Holz, D., Reaction bonding of aluminum oxide (RBAO). *J. Ceram. Soc. Jpn.*, 1995, **103**, 738–745.
6. Snel, M. D., de With, G., Snijkers, F., Luyten, J. and Kodentsov, A., Aqueous tape casting of reaction bonded aluminium oxide (RBAO). *J. Eur. Ceram. Soc.*, 2007, **27**, 27–33.
7. Luyten, J., Thijs, I., Vandermeulen, W., Mullens, S., Wallaeys, B. and Mortelmans, R., Strong ceramic foams from polyurethane templates. *Adv. Appl. Ceram.*, 2005, **104**(1), 4–8.
8. Claussen, N., Janssen, R. and Garcîa, D., Production of an aluminide containing ceramic moulding. German Patent DE 4,447,130, 1996.
9. Chattopadhyay, G. and Kleykamp, H., Phase equilibria and thermodynamic studies in the titanium–nickel and titanium–nickel–oxygen systems. *Z. Metallkde*, 1983, **74**(H. 3), 182–187.
10. Burkes, D. E., Gottoli, G. and Moore, J. J., Mechanical properties of porous combustion synthesized $Ni_3Ti$–$TiC_x$ composites. *Compos. Sci. Technol.*, 2006, **66**, 1931–1940.
11. Vorobey, A. Y. and Guo, C., Femtosecond laser structuring of titanium implants. *Appl. Surf. Sci.*, 2007, **253**, 7272–7280.
12. Wang, H. M. and Liu, Y. F., Microstructure and wear resistance of laser clad $Ti_5Si_3$/$NiTi_2$ intermetallic composite coating on titanium alloy. *Mater. Sci. Eng. A*, 2002, **338**, 126–132.
13. Roosen, A., Basic requirements for tape casting of ceramic powders. In *Ceramics Transactions*, *Vol. 1B*, ed. G. L. Messing, E. R. Fuller and H. Hausner. American Ceramic Society, 1988, pp. 675–692.
14. Tian, T., Jiang, D., Zhang, J. and Lin, Q., Aqueous tape casting process for hydroxyapatite. *J. Eur. Ceram. Soc.*, 2007, **27**, 2671–2677.
15. Uemura, S. and Takayanagi, M., Application of the theory of elasticity and viscosity of two-phase systems to polymer blends. *J. Appl. Polym. Sci.*, 1966, **10**, 113–125.
16. Lungu, A., Mejiritski, A. and Neckers, D. C., Solid state studies on the effect of fillers on the mechanical behaviour of photocured composites. *Polymer*, 1998, **39**(20), 4757–4763.
17. Nielsen, L. E., *Mechanical properties of polymers and composites*, *Vol. 2*. Marcel Dekker Inc., New York, 1974.
18. Leite, M. H. and Ferland, F., Determination of unconfined compressive strength and Young's modulus of porous materials by indentation tests. *Eng. Geol.*, 2001, **59**, 267–280.
19. Gillam, E. and Holden, J. P., Structure of nickel oxide containing alumina. *J. Am. Ceram. Soc.*, 1963, **46**(12), 601–604.
20. Valeeva, A. A., Rempel, A. A. and Gusev, A. I., Ordering of cubic titanium monoxide into monoclinic $Ti_5O_5$. *Inorg. Mater.*, 2001, **37**(6), 603–612.
21. Banus, M. D., Reed, T. B. and Strauss, A. J., Electrical and magnetic properties of TiO and VO. *Phys. Rev. B: Solid State*, 1972, **5**(8), 2775–2784.
22. Snel, M. D., Snijkers, F., Luyten J., Kodentsov, A. and de With, G., Influence of processing on the properties and microstructure of $NiTi_2$–$Ni_3Ti$–TiO composites. *J. Eur. Ceram. Soc.*, in preparation.